

Portfolio Reinforcement Learning with Scenario-Context Rollout

Vanya Priscillia Bendatu
National University of Singapore
vanyabendatu@u.nus.edu

Yao Lu
National University of Singapore
luyao@comp.nus.edu.sg

Abstract

Market regime shifts induce distribution shifts that can degrade the performance of portfolio rebalancing policies. We propose macro-conditioned scenario-context rollout (SCR) that generates plausible next-day multivariate return scenarios under stress events. However, doing so faces new challenges, as history will never tell what would have happened differently. As a result, incorporating scenario-based rewards from rollouts introduces a reward–transition mismatch in temporal-difference learning, destabilizing RL critic training.

We analyze this inconsistency and show it leads to a mixed evaluation target. Guided by this analysis, we construct a counterfactual next state using the rollout-implied continuations and augment the critic agent’s bootstrap target. Doing so stabilizes the learning and provides a viable bias-variance tradeoff.

In out-of-sample evaluations across 31 distinct universes of U.S. equity and ETF portfolios, our method improves Sharpe ratio by up to 76% and reduces maximum drawdown by up to 53% compared with classic and RL-based portfolio rebalancing baselines.

1 Introduction

The financial market is non-stationary. Over time, the expected returns, volatilities, and cross-asset dependency change as the macroeconomic structure and the market dynamics evolve. In portfolio management and rebalancing applications, regime changes may cause degraded returns due to the dependencies during downturns [1–3]. A real-world portfolio policy must be resilient to distribution shifts and synchronized sell-offs [4–6].

Risk management traditionally addresses robustness through scenario analysis and stress testing. Agent-based macro modeling and simulation [7, 8] push this idea further such that policies can be evaluated under counterfactual scenarios while preserving economically meaningful structures. On the other hand, reinforcement learning (RL) enables portfolio

rebalancing and treats the asset allocation problem as a Markov decision process (MDP), aiming to maximize the return while following trading limits and constraints [9–12]. Recent policy-gradient methods, such as proximal policy optimization (PPO) [13], stabilize training with clipped objectives and bootstrapped value targets.

In this paper, we draw inspiration from agent-based macro modeling and explore this idea in training RL agents for portfolio management. To improve next-state estimation, we propose Scenario-Context Rollout (SCR), a leak-safe feedback mechanism to produce a distribution of next-day joint returns under potential economic shocks. However, doing so poses a key technical challenge: while outcomes can be evaluated under plausible simulated scenarios, the agent observes only the realized transitions from the market history and cannot interact with the market to test what-if actions [4]. As a result, alternative trajectories are only hypothetical. This problem worsens in distribution shifts; the policy may generate state and action pairs that are not supported by economic structures [6, 14].

To deepen our comprehension of this problem, we in theory formalize scenario-conditioned learning with historical market data and show that coupling scenario-based rewards with tape-based (realized history) continuations induces hybrid Bellman operator [15, 16] under outcome-dependent state memory and causes a reward–transition mismatch in temporal-difference (TD) learning. Accordingly, we use the Wasserstein-form operator bounds [17, 18] to prove that this hybrid operator generally has a distinct fixed point from the scenario-consistent objective, creating an inherent fixed-point bias. This divergence is not only a nuisance but also exposes a bias–variance tradeoff in critic training.

Based on this analysis, we propose to augment the critic’s bootstrap target with a counterfactual continuation that is constructed from the SCR returns. The resulting target interpolates between a tape and a scenario bootstrap; we show that doing so improves training stability and robustness while adhering to

economic structure and historical observations.

We evaluate our solution on day-to-day portfolio rebalancing across 31 distinct universes of U.S. equity and ETF portfolios. We compare against classic portfolio rebalancing algorithms, tape-only PPO, risk-penalized, and rollout-based baselines. Results show that our solution improves out-of-sample Sharpe ratio by up to 76% and reduces maximum drawdown by over 53%, while providing a more stable RL training.

Contributions of this paper can be summarized as follows:

- We introduce SCR for RL-based portfolio management. SCR is a macroeconomics-guided feedback mechanism that produces a distribution of returns under economic shock scenarios.
- We analyze in theory that scenario rewards together with tape continuations induce a hybrid Bellman operator and yield a fixed-point bias characterized by Wasserstein-form bounds. This implies a bias-variance tradeoff in critic training. We design our solution based on this analysis.
- Our solution shows empirical gains using historical market data over state-of-the-art portfolio rebalancing algorithms and RL models.

2 Method

Rebalancing close-to-close trading portfolios is a sequential decision problem. At the close of every trading day t , we pick a vector of weights $\mathbf{w}_t \in \mathbb{R}^N$ across N assets. To calculate the performance of the portfolio, we use the asset return vector $\mathbf{r}_{t+1} \in \mathbb{R}^N$. Each individual element $r_{t+1,i}$ of this vector is defined as

$$r_{t+1,i} := \frac{p_{t+1,i} - p_{t,i}}{p_{t,i}}, \quad i = 1, \dots, N, \quad (1)$$

where $p_{t,i}$ represents the closing price of asset i on day t . The final realized net portfolio return is then given by

$$R_{p,t+1} = \mathbf{w}_t^\top \mathbf{r}_{t+1} - \text{cost}_t, \quad (2)$$

where cost_t is a term that increases with portfolio turnover [19, 20].

Figure 1 summarizes our scenario-conditioned RL pipeline. We follow the standard PPO actor-critic training paradigm [13] and utilize a learned value function together with a critic bootstrap target. Our objective is to enhance robustness in the face of regime shifts and changes in distribution.

Specifically, we gather regime/exposure features which serve as a retrieval descriptor denoted by ψ_t . Crucially, ψ_t excludes portfolio-history components (e.g., previous weights or internal memory states),

ensuring that scenario retrieval relies solely on market conditions instead of the agent’s past trajectory. Therefore, Scenario-Context Rollout (SCR) estimates a conditional distribution $P_{\text{scen}}(\cdot | \psi_t)$ over next-day joint return vectors induced by macro scenarios. Let $\mathbf{R}_{t+1} \sim P_{\text{scen}}(\cdot | \psi_t)$ denote a generic macro scenario draw. To approximate expectations, we sample independent and identically distributed (i.i.d.) macro scenarios

$$\mathbf{R}_{t+1}^{(s)} \stackrel{\text{i.i.d.}}{\sim} P_{\text{scen}}(\cdot | \psi_t), \quad s = 1, \dots, S.$$

We define $\bar{\mathbf{r}}_{t+1}^{\text{scen}}$ as a compact representation used in the counterfactual continuation (Sec. 2.2). This joint-return, conditioned by the prevailing regime, captures the dependencies and tail risks that become prominent in times of stress.

At each decision time t , the policy observes an input state $\phi_t = (z_t, h_t)$ containing only information available by time t . In this context, z_t encompasses market features and portfolio history and h_t provides longer-horizon context including SCR outputs. The policy model generates an action a_t . To ensure that the final portfolio is valid, we apply a set of operational constraints \mathcal{W}_t , covering box, leverage, and turnover constraints:

$$\mathbf{w}_t = \Pi_t(a_t) \in \mathcal{W}_t, \quad (3)$$

where Π_t denotes the projection onto \mathcal{W}_t . All constraint budgets are treated as held identical across all strategies.

Let $r(\phi, \mathbf{w}; \mathbf{x})$ denote the per-step reward evaluated at state ϕ using weights \mathbf{w} and based on an input return vector \mathbf{x} . We train PPO to maximize a discounted objective where rewards are evaluated under SCR macro scenarios, which involve a conditional distribution of plausible next-day joint returns:

$$J_{\text{scen}}(\pi) := \mathbb{E}_{\pi, P_{\text{scen}}} \left[\sum_{t=0}^{T-1} \delta^t r(\phi_t, \mathbf{w}_t; \mathbf{R}_{t+1}) \right]. \quad (4)$$

The concrete form of reward $r(\phi_t, \mathbf{w}_t; \mathbf{R}_{t+1})$ is defined in Sec. 2.2. We use a discount factor $\delta \in (0, 1)$ to ensure stability in temporal-difference (TD) bootstrapping. That is, in discounted MDPs, the Bellman operator acts as a contraction with a modulus of δ . This enhances the conditioning of value targets and mitigates sensitivity to noise arising from long-horizon estimations (e.g., [12, 21]).

It is important to recognize that a logged market tape (i.e., a fixed, non-rewinding historical record) provides only a single realized next-day return vector \mathbf{r}_{t+1} at each time t , and thus only a single realized continuation. By utilizing executed weights \mathbf{w}_t , we update the realized next state through function $\phi_{t+1} = \text{Upd}(\phi_t, \mathbf{w}_t, \mathbf{r}_{t+1})$. Conversely, Eq. (4)

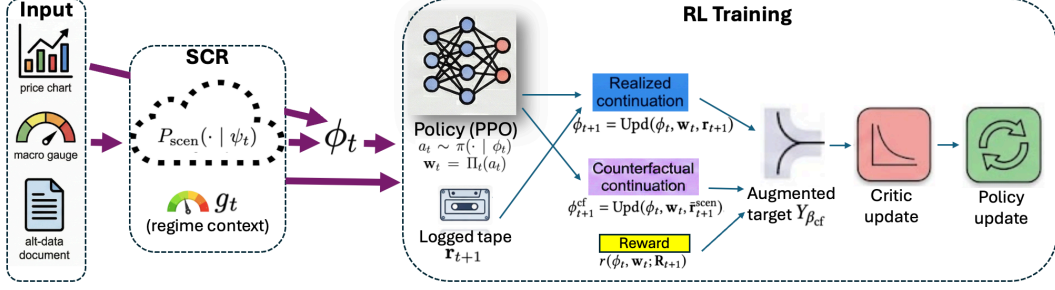


Figure 1: **Overview of our RL paradigm.** SCR produces a conditional scenario distribution over next-day joint return vectors. The critic is trained using a bootstrap target that augments the realized continuation bootstrap with a counterfactual continuation.

specifies *how actions are scored* in macro scenario estimation, but the logged tape determines the realized continuation. This creates a mismatch between (i) scenario-based reward scoring (as in $J_{\text{scen}}(\pi)$) and (ii) the realized next-state transition ϕ_{t+1} . We fix the gap here using the macro scenario conditional mean $\bar{\mathbf{r}}_{t+1}^{\text{scen}}$ by constructing a counterfactual continuation: $\phi_{t+1}^{\text{cf}} = \text{Upd}(\phi_t, \mathbf{w}_t, \bar{\mathbf{r}}_{t+1}^{\text{scen}})$, and then mixing the critic bootstraps evaluated at ϕ_{t+1} and ϕ_{t+1}^{cf} in the augmented TD target $Y_{\beta_{\text{cf}}}$ (see Sec. 2.2). This results in a bootstrap signal that is aligned with the scenario and exhibits low variance, while remaining grounded in the tape. Ultimately, PPO updates the critic based on $Y_{\beta_{\text{cf}}}$ and updates the policy accordingly.

2.1 Scenario-Context Rollout (SCR)

Regime representation. Each trading day t can be represented by a low-dimensional *regime embedding* $U_t \in \mathbb{R}^k$ to summarize the market. U_t is learned to capture patterns in two sources of information: (i) market-macro behavior (cross-sectional returns and macro shocks) and (ii) policy-text signals. Intuitively, nearby points in the shock space correspond to days with similar “macro-financial regimes.” A *shock day* is hence a day whose regime embedding U_t contains an anomaly; this can be learned during training as a binary indicator $\text{shock}_t \in \{0, 1\}$.

As shocks often happen sequentially, spanning days to months. We cluster subsequent shock days into a *shock channel*, assigning each shock-day embedding to an existing cluster or creates a new one when it is farther than a distance threshold λ^2 from all existing *channel centroids* using the running mean embedding of each channel. We keep a *ShockLedger*, a compact catalog of shock channels that encapsulates the channel’s macro signature and representative movers. To obtain a *daily* regime characteristic for conditioning, we aggregate recent channel hits into a binary activation pattern, considering the activated channels as

active near time t . This yields a channel-activation vector $\chi_t \in \{0, 1\}^C$, where $\chi_{t,c} = 1$ if and only if channel c is assigned to at least one shock day within a brief trailing lookback window concluding at time t . The lookback aggregation reflects the enduring effects of macro shocks over several days. This reduces daily fluctuations in the output of the detector, resulting in a more stable conditioning signal.

Scenario retrieval and rollout. Macro scenario retrieval is facilitated through channel activations using ψ_t with the preprocessed regime and exposure data that is accessible at time t (e.g., macro shocks, channel activations χ_t , and exposure summaries). To uphold leak-safety, ψ_t keeps only necessary features and omits those related to the portfolio history. Hence, SCR maintains a library of return vectors indexed by a series of historical decision times \mathcal{I} :

$$\mathcal{D} := \{(\tilde{\mathbf{r}}_{u+1}, \psi_u)\}_{u \in \mathcal{I}}, \quad (5)$$

where $u < t$ denotes a past decision time. The vector $\tilde{\mathbf{r}}_{u+1}$ is a one-step-ahead *macro scenario return* that is derived from the macro context through a rolling macro-to-return map, using only information available at time u .

At time t , SCR restricts to past indices $\mathcal{I}_t := \{u \in \mathcal{I} : u < t\}$ and retrieves nearest neighbors by comparing the current descriptor ψ_t and past descriptors $\{\psi_u\}_{u \in \mathcal{I}_t}$ in \mathcal{D} . Let $\text{sim}(\cdot, \cdot)$ be a similarity score. We define the k nearest-neighbor indices as

$$\mathcal{N}_k(t) := \text{TopK}_{u \in \mathcal{I}_t} \text{sim}(\psi_t, \psi_u). \quad (6)$$

Therefore, SCR produces the conditional distribution based on the retrieval:

$$P_{\text{scen}}(\cdot | \psi_t) := \frac{1}{|\mathcal{N}_k(t)|} \sum_{u \in \mathcal{N}_k(t)} \delta_{\tilde{\mathbf{r}}_{u+1}}(\cdot), \quad (7)$$

where δ_x denotes a point mass at x . During RL training, we draw S i.i.d. macro scenarios $\{\mathbf{R}_{t+1}^{(s)}\}_{s=1}^S$ from $P_{\text{scen}}(\cdot | \psi_t)$.

Regime context g_t . Beyond scenario sampling, SCR outputs a regime context g_t that gates risk-taking at decision time t . It acts as a risk-budget multiplier: $g_t \approx 1$ corresponds to normal conditions, while smaller g_t indicates stress and shrinks scenario-evaluated portfolio payoffs, discouraging aggressive exposures. We compute a nonnegative severity score v_t via a short-horizon deterministic *macro stress rollout* driven by the active channels $\boldsymbol{\chi}_t$, tracking the peak Mahalanobis [22] stress along the rollout. We then normalize v_t against a trailing quantile baseline, as it may drift over time.

Definition 2.1 (Quantile-normalized regime context g_t). Let $v_t \geq 0$ be the severity score at decision time t , and let $\mathcal{W}_t := \{t - L_g, \dots, t - 1\}$ be a trailing window of past decisions of length L_g and a quantile $q_g \in (0, 1)$. Define the reference scale $q_t := \text{Quantile}_{q_g}(\{v_u : u \in \mathcal{W}_t\})$, and the regime context

$$g_t := \text{clip}\left(1 - \alpha_g \frac{v_t}{q_t + \varepsilon}, \underline{g}, 1\right) \in [\underline{g}, 1], \quad (8)$$

where $\alpha_g > 0$ controls sensitivity, $\underline{g} \in (0, 1)$ sets a minimum value. We apply g_t as an *exposure gate* by scaling scenario portfolio returns

$$\tilde{u}_{t+1}^{(s)} = g_t \langle \mathbf{w}_t, \mathbf{R}_{t+1}^{(s)} \rangle,$$

so larger estimated severity (larger v_t) yields smaller g_t , attenuating the reward signal during periods of stress. In other words, it reduces risk-taking and provides smooth, effective risk management.

2.2 Counterfactual Continuation for Critic Target Augmentation

We use a deterministic function $\text{Upd} : (\phi_t, \mathbf{w}_t, \mathbf{x}_{t+1}) \mapsto \phi_{t+1}$, which advances the current state when fed with an *input* return vector $\mathbf{x}_{t+1} \in \mathbb{R}^N$.¹ At time t , the agent selects an action a_t and executes feasible portfolio weights $\mathbf{w}_t = \Pi_t(a_t)$. The tape provides the realized return vector \mathbf{r}_{t+1} and the realized continuation

$$\phi_{t+1} = \text{Upd}(\phi_t, \mathbf{w}_t, \mathbf{r}_{t+1}), \quad \mathbf{r}_{t+1} \text{ from tape.} \quad (9)$$

This realized continuation mismatches with macro scenario estimates. We address this problem by constructing a *counterfactual continuation* and augmenting the critic’s one-step bootstrap target. Specifically, given executed weights \mathbf{w}_t and macro scenario samples

¹ \mathbf{x}_{t+1} is a placeholder for the return vector; on the tape we observe $\mathbf{x}_{t+1} = \mathbf{r}_{t+1}$.

$\{\mathbf{R}_{t+1}^{(s)}\}_{s=1}^S \sim P_{\text{scen}}(\cdot | \psi_t)$, we use the gated outcomes $\tilde{u}_{t+1}^{(s)}$ defined in Sec. 2.1 and their sample mean

$$\bar{u}_{t+1} := \frac{1}{S} \sum_{s=1}^S \tilde{u}_{t+1}^{(s)}.$$

Integrating these macro scenario outcomes yields a risk-aware reward:

$$r_t := \bar{u}_{t+1} - \lambda_\rho \left(\text{Risk}_\eta \left(\{\tilde{u}_{t+1}^{(s)}\}_{s=1}^S \right) + \eta \varepsilon \right) - \text{Reg}(\mathbf{w}_t, \mathbf{w}_{t-1}), \quad (10)$$

where $\lambda_\rho \geq 0$ regulates the intensity of the tail-risk penalty, Risk_η represents a functional that is sensitive to tail conditions with a temperature parameter of $\eta > 0$, and Reg accounts for trading frictions as well as structural penalties.

The conditional mean return is hence approximated through Monte Carlo [23]:

$$\bar{\mathbf{r}}_{t+1}^{\text{scen}} := \mathbb{E}_{P_{\text{scen}}(\cdot | \psi_t)}[\mathbf{R}_{t+1}] \approx \frac{1}{S} \sum_{s=1}^S \mathbf{R}_{t+1}^{(s)}. \quad (11)$$

Using this approximation, we establish the counterfactual continuation by applying the same update function to $\bar{\mathbf{r}}_{t+1}^{\text{scen}}$:

$$\phi_{t+1}^{\text{cf}} = \text{Upd}(\phi_t, \mathbf{w}_t, \bar{\mathbf{r}}_{t+1}^{\text{scen}}). \quad (12)$$

Notably, this counterfactual continuation is secured against data leakage as it relies solely on quantities available by time t . It is also aligned with macro scenario since $\bar{\mathbf{r}}_{t+1}^{\text{scen}}$ is derived from the same macro scenario distribution $P_{\text{scen}}(\cdot | \psi_t)$ utilized for the reward.

Augmenting Critic Bootstrap Target. Let $V_\omega(\phi)$ denote the critic, i.e., a parametric approximation to the state-value function under policy. Let $\delta \in (0, 1)$ be the RL discount factor. Using the same scenario-based reward r_t from Eq. (10), let the one-step targets using (1) the tape-based realized continuation and (2) the counterfactual continuation respectively be

$$Y_r := r_t + \delta V_\omega(\phi_{t+1}), \quad Y_c := r_t + \delta V_\omega(\phi_{t+1}^{\text{cf}}).$$

Therefore we augment the critic target using

$$Y_{\beta_{cf}} = (1 - \beta_{cf}) Y_r + \beta_{cf} Y_c, \quad \beta_{cf} \in [0, 1], \quad (13)$$

where β_{cf} interpolates between tape-faithful bootstrapping and scenario-aligned bootstrapping. The critic is trained by regressing $V_\omega(\phi_t)$ onto $Y_{\beta_{cf}}$, and the policy model undergoes updates through PPO-Clip with GAE advantages (Alg. 1).

Algorithm 1 Actor-critic training using logged tape with SCR macro scenarios and augmented targets

Require: Logged tape $\{\phi_t, \mathbf{r}_{t+1}\}_{t=0}^{T-1}$; SCR module returning $(P_{\text{scen}}(\cdot | \psi_t), g_t)$; feasibility map Π_t ; update Upd ; discount δ ; mixing β_{cf} ; scenario sample size S

- 1: **for** each iteration of PPO update **do**
- 2: **for** $t = 0, \dots, T-1$ (traverse through logged dates) **do**
- 3: Construct ϕ_t ; sample $a_t \sim \pi_\theta(\cdot | \phi_t)$; $\mathbf{w}_t = \Pi_t(a_t)$
- 4: Obtain $(P_{\text{scen}}(\cdot | \psi_t), g_t)$ from the SCR module
- 5: Sample $\{\mathbf{R}_{t+1}^{(s)}\}_{s=1}^S \sim P_{\text{scen}}(\cdot | \psi_t)$
- 6: Compute scenario reward r_t using $\{\mathbf{R}_{t+1}^{(s)}\}$, g_t (Eq. (10))
- 7: Compute scenario mean $\bar{\mathbf{r}}_{t+1}^{\text{scen}} = \frac{1}{S} \sum_{s=1}^S \mathbf{R}_{t+1}^{(s)}$ (Eq. (11))
- 8: Read realized \mathbf{r}_{t+1} from tape; $\phi_{t+1} = \text{Upd}(\phi_t, \mathbf{w}_t, \mathbf{r}_{t+1})$
- 9: Set $\phi_{t+1}^{\text{cf}} = \text{Upd}(\phi_t, \mathbf{w}_t, \bar{\mathbf{r}}_{t+1}^{\text{scen}})$ (Eq. (12))
- 10: Form augmented target $Y_{\beta_{cf}}$ using Eq. (13)
- 11: **end for**
- 12: Update critic by regressing $V_\omega(\phi_t)$ onto $Y_{\beta_{cf}}$
- 13: Compute Generalized Advantage Estimation \hat{A}_t
- 14: Update actor using PPO-Clip with \hat{A}_t
- 15: **end for**

3 Continuation Mismatch and Fixes

This section discusses the *continuation mismatch* at the Bellman operator level [12, 15, 21, 24] and explains why *augmenting targets on the critic side* is both adequate and well-founded.

Hybrid vs. scenario-consistent operators. Let a policy π be defined along with any bounded value function V . According to Sec. 2, ψ be the leak-safe descriptor used by SCR and $P_{\text{scen}}(\cdot | \psi)$ for the induced scenario return law. Let $P_{\text{real}}(\cdot | \phi)$ denote the (conceptual) real-world conditional return law for the tape outcome.

We consider two Bellman-style operators that differ only in their bootstrapping techniques: the *hybrid* operator evaluates *scenario reward* but bootstraps on the *realized continuation*, while the *scenario-consistent* operator uses scenario outcomes for both reward and continuation:

$$(T_{\text{hyb}}^\pi V)(\phi) := \mathbb{E}[r(\phi, \mathbf{w}; \mathbf{R}) + \delta V(\text{Upd}(\phi, \mathbf{w}, \mathbf{r})) | \phi], \quad (14)$$

where $a \sim \pi(\cdot | \phi)$, $\mathbf{w} = \Pi(a)$, $\mathbf{R} \sim P_{\text{scen}}(\cdot | \psi)$, and $\mathbf{r} \sim P_{\text{real}}(\cdot | \phi)$. In contrast,

$$(T_{\text{scen}}^\pi V)(\phi) := \mathbb{E}[r(\phi, \mathbf{w}; \mathbf{R}) + \delta V(\text{Upd}(\phi, \mathbf{w}, \mathbf{R})) | \phi], \quad (15)$$

with the same action sampling but using the scenario outcome within its continuation. Thus T_{hyb}^π corresponds to *scenario reward + realized continuation*, while T_{scen}^π corresponds to *scenario reward + scenario continuation*. When Upd depends on the newly observed next-day return via the memory component h and $P_{\text{scen}}(\cdot | \psi) \neq P_{\text{real}}(\cdot | \phi)$, these operators typically converge to different fixed points. This is because they take evaluation of the continuation term $V(\text{Upd}(\phi, \mathbf{w}, \cdot))$ under different outcome distributions.

Lemma 3.1. Fix ϕ and take any bounded V . We define the function

$$f_{\phi, a}(\mathbf{x}) := V(\text{Upd}(\phi, \Pi(a), \mathbf{x})). \quad (16)$$

Then for any policy π ,

$$\begin{aligned} (T_{\text{hyb}}^\pi V - T_{\text{scen}}^\pi V)(\phi) &= \delta \mathbb{E}_{a \sim \pi(\cdot | \phi)} [\Delta(\phi, \psi, a)], \\ \Delta(\phi, \psi, a) &:= \mathbb{E}_{\mathbf{r} \sim P_{\text{real}}(\cdot | \phi)} [f_{\phi, a}(\mathbf{r})] \\ &\quad - \mathbb{E}_{\mathbf{R} \sim P_{\text{scen}}(\cdot | \psi)} [f_{\phi, a}(\mathbf{R})]. \end{aligned} \quad (17)$$

Proposition 3.2. Assume that for each fixed (ϕ, \mathbf{w}) the map $\mathbf{x} \mapsto \text{Upd}(\phi, \mathbf{w}, \mathbf{x})$ is L_h -Lipschitz in \mathbf{x} through the outcome-updated memory component h , i.e., $\|h(\text{Upd}(\phi, \mathbf{w}, \mathbf{x})) - h(\text{Upd}(\phi, \mathbf{w}, \mathbf{y}))\| \leq L_h \|\mathbf{x} - \mathbf{y}\|_2$. Also, assume V is L_V -Lipschitz in that memory (holding exogenous context fixed). Let o denote the information available at the decision time, $\phi = \Phi(o)$ and $\psi = \Psi(o)$ be summaries constructed from the same o . Let $\delta \in (0, 1)$ denote the discount factor used in the operators.

Define the mismatch by

$$\Delta_W := \sup_o W_1(P_{\text{real}}(\cdot | \Phi(o)), P_{\text{scen}}(\cdot | \Psi(o))), \quad (18)$$

where W_1 is the 1-Wasserstein distance with ground metric $d(\mathbf{x}, \mathbf{y}) = \|\mathbf{x} - \mathbf{y}\|_2$ [25]. Then for any policy π and any such V , the resulting one-step operator deviation is bounded by

$$\|T_{\text{hyb}}^\pi V - T_{\text{scen}}^\pi V\|_\infty \leq \delta L_V L_h \Delta_W. \quad (19)$$

Corollary 3.3. Let V_{scen}^π be the fixed point of T_{scen}^π and V_{hyb}^π be the fixed point of T_{hyb}^π , assuming both are δ -contractions on $(\mathcal{V}, \|\cdot\|_\infty)$. Assume V_{scen}^π is L_V -Lipschitz in the outcome-updated memory component h , and define

$$L_V := \text{Lip}_h(V_{\text{scen}}^\pi).$$

Under the conditions of Proposition 3.2,

$$\|V_{\text{hyb}}^\pi - V_{\text{scen}}^\pi\|_\infty \leq \frac{\delta}{1-\delta} L_V L_h \Delta_W, \quad (20)$$

with Δ_W from (18).

A conflict inherent to logged tape learning is shown in Corollary 3.3. Applying macro scenarios directly to the reward creates immediate friction with the critic. The fundamental problem is that we are scoring actions under SCR macro scenarios, even though we still depend on the tape for bootstrapping. Consequently, the TD update gradually deviates. It follows the *hybrid* operator and converges (in expectation) to V_{hyb}^π , not to the scenario-consistent value, V_{scen}^π , required by the scoring objective J_{scen} (Eq. (4)). Lemma 3.1 isolates the core issue, showing that the mismatch stems entirely from the continuation term. This is a crucial detail since it means we can adjust the critic bootstrap without actually interfering with the tape traversal. We resolve the issue by generating a counterfactual continuation state and combining its value with the realized tape bootstrap. This creates an augmented target that reduces the mismatch. As a result, following the logic in Sec. 2.2, we can rectify the critic while ensuring our rollouts strictly faithful to the tape.

Assumption 3.4. Let $\phi = (z, h)$, where h is the outcome-updated memory component and z denotes exogenous context. For any fixed (ϕ, \mathbf{w}) , assume the update map $\mathbf{x} \mapsto \text{Upd}(\phi, \mathbf{w}, \mathbf{x})$ is L_h -Lipschitz in \mathbf{x} through h . Likewise, the scenario-consistent value V_{scen}^π is L_V -Lipschitz in h (holding z fixed). Finally, the mismatch and proxy second moments are assumed to be finite:

$$\begin{aligned} W_2^2(P_{\text{real}}(\cdot | \phi), P_{\text{scen}}(\cdot | \psi)) &< \infty, \\ \mathbb{E}[\|\mathbf{R} - \mu_\psi\|_2^2 | \psi] &< \infty, \end{aligned}$$

where $\mathbf{R} \sim P_{\text{scen}}(\cdot | \psi)$ and $\mu_\psi := \mathbb{E}[\mathbf{R} | \psi]$.

We bound the one-step mean squared error between the augmented target and the scenario-consistent target Y^* in accordance with Assumption 3.4.

Theorem 3.5 (One-step mixing bound (Wasserstein form)). *Consider a decision time with state ϕ , descriptor ψ , and a raw action a with executed control $\mathbf{w} = \Pi(a)$. Let the scenario-consistent one-step target be*

$$\begin{aligned} Y^* &:= r(\phi, \mathbf{w}; \mathbf{R}) + \delta V_{\text{scen}}^\pi(\text{Upd}(\phi, \mathbf{w}, \mathbf{R})), \\ \mathbf{R} &\sim P_{\text{scen}}(\cdot | \psi). \end{aligned}$$

Define $Y_{\beta_{\text{cf}}}$ as in (13) using V_{scen}^π in place of V_ω and $\phi^{\text{cf}} = \text{Upd}(\phi, \mathbf{w}, \mu_\psi)$. Under Assumption 3.4, define

$$\begin{aligned} \Delta_2(\phi, \psi) &:= W_2^2(P_{\text{real}}(\cdot | \phi), P_{\text{scen}}(\cdot | \psi)), \\ \sigma_{\text{scen}}^2(\psi) &:= \mathbb{E}[\|\mathbf{R} - \mu_\psi\|_2^2 | \psi]. \end{aligned}$$

Then

$$\begin{aligned} &\mathbb{E}[(Y_{\beta_{\text{cf}}} - Y^*)^2 | \phi, \psi, a] \\ &\leq 2\delta^2(L_V L_h)^2 \left((1-\beta_{\text{cf}})^2 \Delta_2(\phi, \psi) + \beta_{\text{cf}}^2 \sigma_{\text{scen}}^2(\psi) \right). \end{aligned} \quad (21)$$

Corollary 3.6. Let $A(\phi, \psi) := \Delta_2(\phi, \psi)$ denote the mismatch and $B(\psi) := \sigma_{\text{scen}}^2(\psi)$ the proxy variance. Minimizing the right hand side of (21) yields the optimal mixing weight:

$$\beta_{\text{cf}}^*(\phi, \psi) = \frac{A(\phi, \psi)}{A(\phi, \psi) + B(\psi)} \in [0, 1]. \quad (22)$$

Critic target augmentation is a bias–variance tradeoff. By weighing the mismatch error, $(1 - \beta_{\text{cf}})^2 \Delta_2$, against the proxy variance, $\beta_{\text{cf}}^2 \sigma_{\text{scen}}^2$, the bound reveals a clear tension. Corollary 3.6 suggests that a “sweet spot” exists whenever both error sources are significant, mirrors the empirical trends for β_{cf} seen in Sec. 4.4.

4 Experiments

We evaluate our method on the daily close-to-close portfolio rebalancing task to demonstrate the effectiveness and robustness of our solution, particularly in regime mixture changes.

4.1 Experimental Setup

Datasets and universe construction. We use the FinRL U.S. equities and ETFs dataset covering 2009–2023 [26]. Across all experiments, we enforce a chronological split: Training (2009–2017), Validation (2018–2019), and an out-of-sample Testing (2020–2023). A *universe* is a fixed set of assets (along with their return panels) that we rebalance. To make sure our findings aren’t an artifact of any one asset set, we evaluate on 31 distinct trading universes, each containing roughly 10–20 assets. We evaluate across four categories: Market-Proxy (1 universe of broad market/sector ETFs), High-Vol (10 distinct high-volatility equity universes), Low-Vol (10 distinct low-volatility equity universes), and General (10 distinct equity universes from the broader cross-section) [27, 28].

Table 1: **Evaluations and comparisons of portfolio rebalancing algorithms by universe group.** Values are in median [Q1, Q3].

Universe	Method	Sharpe \uparrow	Calmar \uparrow	AnnVol \downarrow	MaxDD \downarrow	Turnover
High-Vol	1/N	0.618 [0.563, 0.692]	0.912 [0.471, 2.114]	0.635 [0.356, 3.047]	0.445 [0.396, 0.493]	0.0000 [0.0000, 0.0000]
	Markowitz	0.561 [0.476, 0.699]	0.500 [0.317, 0.767]	0.527 [0.258, 0.780]	0.441 [0.411, 0.461]	0.0256 [0.0215, 0.0283]
	Inverse-Vol	0.630 [0.576, 0.695]	0.873 [0.411, 2.363]	0.589 [0.316, 2.350]	0.418 [0.404, 0.480]	0.0175 [0.0169, 0.0182]
	GMV (Ledoit-Wolf)	0.580 [0.533, 0.645]	0.850 [0.305, 1.397]	0.858 [0.518, 1.076]	0.412 [0.365, 0.449]	0.0261 [0.0216, 0.0305]
	PPO (Historical Replay)	0.615 [0.517, 0.719]	1.127 [0.445, 2.451]	0.569 [0.363, 3.674]	0.416 [0.385, 0.498]	0.298 [0.293, 0.299]
	BootRollout-PPO	0.598 [0.535, 0.729]	1.112 [0.502, 2.295]	0.647 [0.331, 3.798]	0.414 [0.367, 0.478]	0.2995 [0.2951, 0.2997]
	SCR-PPO-Full	0.782 [0.628, 0.948]	0.699 [0.519, 1.104]	0.226 [0.199, 0.297]	0.238 [0.187, 0.304]	0.0049 [0.0044, 0.0074]
Low-Vol	1/N	0.086 [0.073, 0.232]	0.001 [-0.006, 0.075]	0.171 [0.158, 0.180]	0.340 [0.321, 0.368]	0.0000 [0.0000, 0.0000]
	Markowitz	-0.084 [-0.155, -0.027]	-0.058 [-0.093, -0.039]	0.137 [0.123, 0.147]	0.333 [0.300, 0.344]	0.0046 [0.0018, 0.0146]
	Inverse-Vol	0.105 [0.041, 0.155]	0.014 [-0.015, 0.042]	0.165 [0.143, 0.172]	0.321 [0.276, 0.326]	0.0143 [0.0133, 0.0152]
	GMV (Ledoit-Wolf)	-0.088 [-0.131, -0.055]	-0.057 [-0.071, -0.038]	0.112 [0.102, 0.117]	0.278 [0.247, 0.295]	0.0274 [0.0215, 0.0292]
	PPO (Historical Replay)	0.079 [0.029, 0.181]	-0.004 [-0.031, 0.046]	0.174 [0.157, 0.183]	0.337 [0.317, 0.369]	0.164 [0.156, 0.294]
	BootRollout-PPO	0.090 [0.054, 0.184]	0.000 [-0.018, 0.050]	0.176 [0.159, 0.184]	0.343 [0.302, 0.372]	0.2995 [0.2993, 0.2998]
	SCR-PPO-Full	0.641 [0.602, 0.707]	0.453 [0.400, 0.569]	0.116 [0.109, 0.121]	0.164 [0.150, 0.186]	0.0049 [0.0046, 0.0052]
General	1/N	0.444 [0.376, 0.468]	0.182 [0.148, 0.197]	0.231 [0.229, 0.235]	0.423 [0.414, 0.433]	0.0000 [0.0000, 0.0000]
	Markowitz	0.434 [0.333, 0.554]	0.167 [0.122, 0.305]	0.223 [0.189, 0.267]	0.387 [0.340, 0.427]	0.0044 [0.0018, 0.0095]
	Inverse-Vol	0.472 [0.440, 0.516]	0.221 [0.200, 0.246]	0.238 [0.222, 0.239]	0.395 [0.370, 0.402]	0.0169 [0.0159, 0.0171]
	GMV (Ledoit-Wolf)	0.200 [0.082, 0.397]	0.063 [0.008, 0.280]	0.148 [0.134, 0.222]	0.329 [0.260, 0.377]	0.0282 [0.0263, 0.0314]
	PPO (Historical Replay)	0.435 [0.341, 0.525]	0.188 [0.136, 0.270]	0.238 [0.231, 0.242]	0.409 [0.399, 0.416]	0.194 [0.158, 0.282]
	BootRollout-PPO	0.419 [0.360, 0.517]	0.188 [0.137, 0.239]	0.232 [0.226, 0.235]	0.400 [0.388, 0.420]	0.2996 [0.2995, 0.2997]
	SCR-PPO-Full	0.900 [0.768, 0.992]	0.972 [0.855, 1.350]	0.171 [0.162, 0.178]	0.167 [0.142, 0.176]	0.0059 [0.0054, 0.0062]
Market-Proxy	1/N	0.508 [0.508, 0.508]	0.250 [0.250, 0.250]	0.225 [0.225, 0.225]	0.371 [0.371, 0.371]	0.0000 [0.0000, 0.0000]
	Markowitz	0.381 [0.381, 0.381]	0.165 [0.165, 0.165]	0.210 [0.210, 0.210]	0.362 [0.362, 0.362]	0.0056 [0.0056, 0.0056]
	Inverse-Vol	0.494 [0.494, 0.494]	0.241 [0.241, 0.241]	0.217 [0.217, 0.217]	0.361 [0.361, 0.361]	0.0091 [0.0091, 0.0091]
	GMV (Ledoit-Wolf)	0.569 [0.569, 0.569]	0.303 [0.303, 0.303]	0.208 [0.208, 0.208]	0.335 [0.335, 0.335]	0.0468 [0.0468, 0.0468]
	PPO (Historical Replay)	0.492 [0.479, 0.523]	0.241 [0.234, 0.268]	0.228 [0.228, 0.228]	0.370 [0.367, 0.372]	0.220 [0.210, 0.267]
	BootRollout-PPO	0.496 [0.481, 0.509]	0.245 [0.238, 0.255]	0.227 [0.226, 0.228]	0.365 [0.364, 0.371]	0.2926 [0.2893, 0.2947]
	SCR-PPO-Full	1.004 [1.001, 1.014]	0.971 [0.928, 0.991]	0.175 [0.173, 0.177]	0.179 [0.176, 0.193]	0.0053 [0.0052, 0.0054]

Evaluation metrics. In line with recent related work in portfolio rebalancing and risk assessment [29–31], we evaluate out-of-sample performance using a set of comprehensive metrics. The assessment of risk-adjusted performance employs the Sharpe ratio and the Calmar ratio, which respectively reflect the average excess return per unit of volatility and drawdown-aware performance. To assess the total risk exposure, we measure annualized volatility (AnnVol), while tail risk is analyzed via maximum drawdown (MaxDD), defined as the largest peak-to-trough loss. Additionally, we report turnover as a measure of trading intensity and implementability, computed as the average ℓ_1 change in portfolio weights. These metrics, taken together, show how returns and risk behave when the market environment changes and the distribution shifts.

Baselines. We compare against both classical portfolio baselines and RL-based solutions. All reported metrics are computed from realized net returns on the held-out out-of-sample test window.

- *Classic portfolio algorithms*, including (i) equal-weight $1/N$ [32, 33], (ii) mean-variance [34, 35], (iii) inverse-volatility weighting [36, 37], and (iv) global minimum-variance (GMV) with Ledoit-Wolf shrinkage [38, 39].
- *PPO (Historical Replay)*: PPO trained only on

realized market transitions, using PPO-Clip [13] with generalized advantage estimation [40].

- *BootRollout-PPO (with historical simulation)*: Inspired by historical simulation [41], we bootstrap S joint return vectors from a trailing window of realized returns (preserving cross-asset co-movements) and score portfolios with a downside-risk-penalized objective (entropic left-tail) [42]; PPO otherwise trains on the same realized tape transitions with standard bootstrapping.
- *SCR-PPO-RewardOnly*: A variant of our solution in which SCR macro scenarios for reward only, with standard tape bootstrapping and without regularization.
- *SCR-PPO-NoCF*: A variant of our solution in which SCR macro scenarios for reward with regularization, but bootstrapping uses realized tape continuation only.
- *SCR-PPO-Full*: SCR macro scenarios for reward with regularization stack and augmented critic bootstrap target ($\beta_{cf} > 0$).

Shock Discovery. SCR conditions applied to the channel-activation vector χ_t confirms the conditioning signal is non-degenerate and exhibits reasonable behaviour in out-of-sample. On Market-Proxy, the detector successfully re-identifies recurring channels in validation and test, producing similar χ_t patterns. No

Table 2: Illustrative ShockLedger channels used in experiments.

Episode Type	Macro Signature	Top Moves	Activity Period
Recurring	Geopolitical/Oil Shock GPR ↑, Brent ↑, Energy ↑	+(XLP, XLV); -(XLF, XLB)	2009–2023 (38 days; 14 in train)
Recurring	Policy Uncertainty GPR ↓, EPU ↑, WTI ↓	+(XLK, XLV); -(XLE, XLF)	2009–2021 (18 days; 16 in train)
Novel (Anomaly)	COVID-19 Liquidity Crisis No training-set channel match Flagged by novelty filter	Detected as novel episode	March 2020 (Consecutive days)

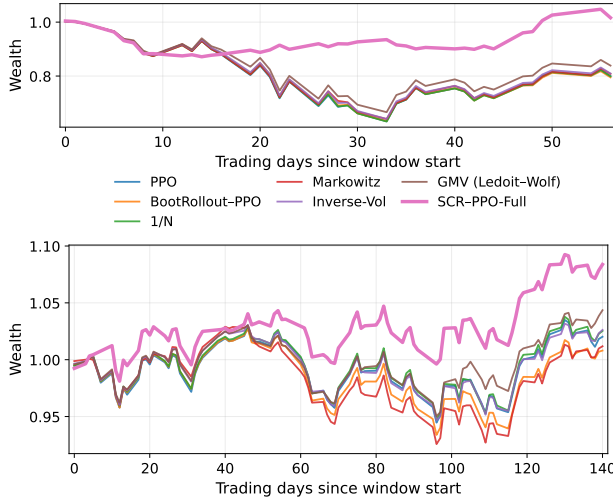


Figure 2: We stress test under shocks. The wealths are rebased to 1 at the window start. Top: COVID-19 sell-off window. Bottom: 2021–2022 macro shock window.

tably, it identifies March 2020 as out-of-support when the lookback window activates channels that were not encountered during training. In instances of novelty detection, SCR resorts to acceptable nearest-neighbor resampling from the available historical data, thereby avoiding retrieval from unrelated episodes. Table 2 presents representative entries from ShockLedger, verifying that regime summaries via χ_t are stable and capable of identifying novel instances outside the existing support. Building on this qualitative verification, we turn to quantitative evaluation to test the effect of regime-local scenario conditioning, including generalization and value learning.

4.2 Evaluation on Out-of-Sample Regimes

Table 1 presents the evaluation metrics for High-Vol, Low-Vol, General, and Market-Proxy groups. SCR-PPO-Full enhances risk-adjusted performance and tail behavior out-of-sample. It stays reliable across different regimes and cross-sectional variations.

In comparison to PPO (Historical Replay), Sharpe

shows consistent increase: 0.615 \rightarrow 0.782 (High-Vol), 0.079 \rightarrow 0.641 (Low-Vol), 0.435 \rightarrow 0.900 (General), and 0.492 \rightarrow 1.004 (Market-Proxy). These enhancements are accompanied by reduced drawdowns (e.g., High-Vol MaxDD 0.416 \rightarrow 0.238, Low-Vol 0.337 \rightarrow 0.164 General 0.409 \rightarrow 0.167, Market-Proxy 0.370 \rightarrow 0.179), along with negligible turnover (\approx 0.004–0.006) in contrast to PPO’s high turnover (\approx 0.15–0.30), suggesting reduced churn without sacrificing downside control.

Qualitative stress-window evidence. On Market-Proxy, Fig. 2 provides a stringent stress test: during two major crisis windows, SCR-PPO-Full protects capital and keeps drawdowns smaller. It also stays more stable throughout the downturn. When markets rebound, it compounds faster than both RL and classical rebalancing baselines. Overall, it achieves higher cumulative returns under sharp regime shifts.

4.3 Ablations and Scenario-to-Real Analysis

To ensure that the scenario–real mismatch and critic stability are observable, we report seed-averaged diagnostics on Market-Proxy. Here, beyond the aggregate metrics in Sec. 4.2, we track diagnostics that correspond to the operator and mixing analysis in Sec. 3. We gauge scenario–real mismatch on held-out dates via scenario-to-real gap $\text{Gap}_{\text{final}} = |\hat{J}_{\text{scen}} - \hat{J}_{\text{real}}|$, where \hat{J}_{scen} is the *cumulative average daily return* over the test dates under SCR scenario scoring and \hat{J}_{real} is the corresponding cumulative average daily return realized on the tape. We summarize critic stability by *Residual-AUC*, the area under the Bellman-residual curve resid_{ℓ_2} versus training progress.

Table 3 demonstrates the results. Relative to PPO trained on Historical Replay, introducing scenario-conditioned training via SCR-PPO-RewardOnly improves pooled out-of-sample robustness: Sharpe increases (0.457 \rightarrow 0.506), drawdowns improve (MaxDD 0.381 \rightarrow 0.168), and turnover drops sharply (0.232 \rightarrow 0.005). SCR also reduces mismatch ($\text{Gap}_{\text{final}}$ 0.526 \rightarrow 3×10^{-4}) and lowers critic error (Resid-AUC 0.217 \rightarrow 0.102), consistent with higher-support scenario conditioning stabilizing value learning on the logged tape.

Our controlled comparison SCR-PPO-NoCF \rightarrow SCR-PPO-Full holds the scenario mechanism and regularization stack fixed and changes only the critic bootstrap target, isolating continuation mismatch (Lemma 3.1). Enabling counterfactual continuation mixing improves pooled risk-adjusted performance (Sharpe 0.647 \rightarrow 0.805, Calmar 0.561 \rightarrow 0.737) and reduces critic error (Resid-AUC 0.087 \rightarrow 0.075). On

Table 3: Ablation study of our solution. We report median values across multiple runs.

Variant	Sharpe	Calmar	AnnVol	MaxDD	Turnover	Gap _{final}	Resid-AUC
PPO (Historical Replay)	0.457 [0.256, 0.543]	0.222 [0.086, 0.335]	0.231 [0.188, 0.347]	0.381 [0.359, 0.414]	0.2320 [0.1600, 0.2983]	0.526 [0.304, 1.882]	0.217 [0.204, 0.231]
SCR-PPO-RewardOnly	0.506 [-0.054, 0.650]	0.364 [0.223, 0.584]	0.127 [0.107, 0.205]	0.181 [0.148, 0.330]	0.0050 [0.0049, 0.0051]	0.0003 [0.0001, 0.0016]	0.102 [0.054, 0.115]
SCR-PPO-NoCF	0.647 [0.571, 0.810]	0.561 [0.379, 0.833]	0.146 [0.110, 0.217]	0.184 [0.158, 0.198]	0.0045 [0.0042, 0.0049]	0.0001 [0.0000, 0.0012]	0.087 [0.077, 0.098]
SCR-PPO-Full	0.805 [0.635, 0.970]	0.737 [0.494, 0.984]	0.171 [0.122, 0.196]	0.179 [0.162, 0.194]	0.0046 [0.0044, 0.0049]	0.0001 [0.0000, 0.0003]	0.075 [0.061, 0.084]

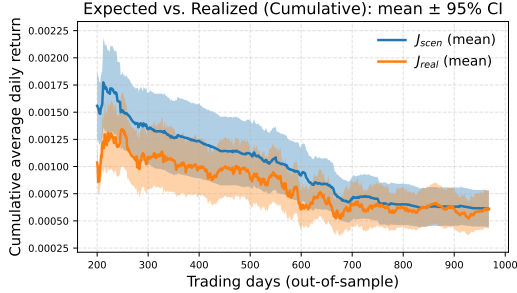


Figure 3: Scenario-to-real validation. Cumulative average daily return under SCR scenario scoring versus realized tape returns.

Learning stability (Contraction): SCR-PPO-Full vs PPO (Historical Replay)

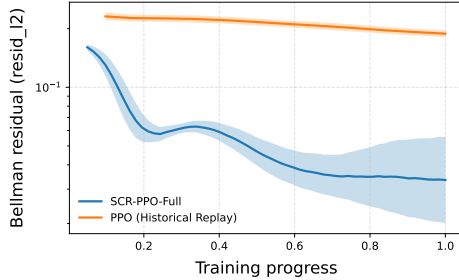


Figure 4: Critic stability under logged-tape mismatch. Bellman residual resid_{ℓ_2} versus training progress (mean \pm 95% CI). Compared to PPO (Historical Replay), SCR-PPO-Full attains smaller residuals, and improved critic stability.

Market-Proxy, we report mean \pm 95% confidence intervals for $\widehat{J}_{\text{scen}}$ and $\widehat{J}_{\text{real}}$ (Fig. 3), and evaluate critic stability via TD-residual contraction (Fig. 4), as motivated by Theorem 3.5. These seed-averaged plots make the mismatch and critic contraction predicted by our theory directly observable (Figs. 3–4).

4.4 Sensitivity Analysis

Counterfactual mixing β_{cf} . We show in Table 4 that using a moderate coefficient results in consistent performance across different universes. In contrast, setting the coefficient in both extremes, i.e., $\beta_{cf} = 0$ uses only continuation mismatch, while $\beta_{cf} = 1$ relies entirely on counterfactual continuation and can amplify approximation error, resulting in degraded performance. This observation aligns with the bias–

Table 4: Sensitivity to β_{cf} . We report median Sharpe here.

Setting	High-Vol	Low-Vol	General	Market-Proxy
$\beta_{cf} = 0.0$	0.736	0.598	0.640	0.821
$\beta_{cf} = 0.25$	0.529	0.529	0.716	0.823
$\beta_{cf} = 0.5$	0.782	0.641	0.900	1.004
$\beta_{cf} = 0.75$	0.518	0.509	0.671	0.838
$\beta_{cf} = 1.0$	0.563	0.584	0.645	0.842

variance trade-off in Theorem 3.5.

5 Conclusion

To improve the return and robustness of reinforcement learning-based portfolio rebalancing, we propose Scenario-Context Rollout (SCR), which is a macroeconomic-guided feedback mechanism to produce scenario returns. To effectively train the RL agent using historical tapes, we analyzed how combining scenario-based rewards with tape-realized transitions induces a continuation mismatch. To address this issue, we augment the critic target using counterfactual continuation; doing so provides a principled bias–variance trade-off and stabilizes critic updates. Our experiments show that the proposed solution improves out-of-sample Sharpe ratios and reduces drawdowns compared with strong baselines. Meanwhile, our solution remains effective across market regimes.

References

- [1] François Longin and Bruno Solnik. Extreme correlation of international equity markets. *The Journal of Finance*, 56(2):649–676, 2001. doi: 10.1111/0022-1082.00340.
- [2] R. A. J. Campbell, Kees G. Koedijk, and Paul Kofman. Increased correlation in bear markets. *Financial Analysts Journal*, 58(1):87–97, 2002. doi: 10.2469/faj.v58.n1.2512.
- [3] Andrew Ang and Joseph Chen. Asymmetric correlations of equity portfolios. *Journal of Financial Economics*, 63(3):443–494, 2002.

- [4] Sergey Levine, Aviral Kumar, George Tucker, and Justin Fu. Offline reinforcement learning: Tutorial, review, and perspectives on open problems. *arXiv preprint arXiv:2005.01643*, 2020.
- [5] Scott Fujimoto, David Meger, and Doina Precup. Off-policy deep reinforcement learning without exploration. In *Proceedings of the 36th International Conference on Machine Learning*, volume 97 of *Proceedings of Machine Learning Research*, pages 2052–2062. PMLR, 2019.
- [6] Aviral Kumar, Aurick Zhou, George Tucker, and Sergey Levine. Conservative q-learning for offline reinforcement learning. In *Advances in Neural Information Processing Systems*, 2020.
- [7] Sebastian Poledna, Michael Gregor Miess, Cars Hommes, and Katrin Rabitsch. Economic forecasting with an agent-based model. *European Economic Review*, 151:104306, 2023.
- [8] Frank Westerhoff and Reiner Franke. Agent-based models for economic policy design. In Shu-Heng Chen, Mak Kaboudan, and Ye-Rong Du, editors, *The Oxford Handbook of Computational Economics and Finance*, pages 603–624. Oxford University Press, 2018.
- [9] John E. Moody and Matthew Saffell. Learning to trade via direct reinforcement. *IEEE Transactions on Neural Networks*, 12(4):875–889, 2001. doi: 10.1109/72.935097.
- [10] Zhengyao Jiang, Dixing Xu, and Jinjun Liang. A deep reinforcement learning framework for the financial portfolio management problem, 2017. URL <https://arxiv.org/abs/1706.10059>.
- [11] Thomas Fischer and Christopher Krauss. Deep learning with long short-term memory networks for financial market predictions. *European Journal of Operational Research*, 270(2):654–669, 2018. doi: 10.1016/j.ejor.2017.11.054.
- [12] Richard S. Sutton and Andrew G. Barto. *Reinforcement Learning: An Introduction*. MIT Press, Cambridge, MA, 2 edition, 2018.
- [13] John Schulman, Filip Wolski, Prafulla Dhariwal, Alec Radford, and Oleg Klimov. Proximal policy optimization algorithms, 2017. URL <https://arxiv.org/abs/1707.06347>.
- [14] Aviral Kumar, Justin Fu, Matthew Soh, George Tucker, and Sergey Levine. Stabilizing off-policy q-learning via bootstrapping error reduction. In *Advances in Neural Information Processing Systems*, 2019.
- [15] Martin L. Puterman. *Markov Decision Processes: Discrete Stochastic Dynamic Programming*. John Wiley & Sons, 1994. ISBN 9780471619772.
- [16] Huizhen Yu, Ashique Rupam Mahmood, and Richard S. Sutton. On generalized bellman equations and temporal-difference learning. *Journal of Machine Learning Research*, 19(47):1–50, 2018. URL <https://www.jmlr.org/papers/v19/17-283.html>.
- [17] Cédric Villani. *Optimal Transport: Old and New*, volume 338 of *Grundlehren der mathematischen Wissenschaften*. Springer, 2008.
- [18] Norman Ferns, Prakash Panangaden, and Doina Precup. Metrics for finite markov decision processes. In *Proceedings of the 20th Conference on Uncertainty in Artificial Intelligence (UAI)*, pages 162–169. AUAI Press, 2004.
- [19] A. V. Olivares-Nadal and V. DeMiguel. Technical note—a robust perspective on transaction costs in portfolio optimization. *Operations Research*, 66(3):733–739, 2018. doi: 10.1287/opre.2017.1699.
- [20] D. Vassallo. *Dynamic Models for Financial and Sentiment Time Series*. PhD thesis, Scuola Normale Superiore, January 2022. URL <https://hdl.handle.net/20.500.14242/167379>.
- [21] Dimitri P. Bertsekas and John N. Tsitsiklis. *Neuro-Dynamic Programming*. Athena Scientific, Belmont, MA, 1996. ISBN 978-1-886529-10-6.
- [22] Prasanta Chandra Mahalanobis. Reprint of: Mahalanobis, p.c. (1936) “on the generalised distance in statistics.”. *Sankhya A*, 80(Suppl 1):1–7, 2018. doi: 10.1007/s13171-019-00164-5.
- [23] Paul Glasserman. *Monte Carlo Methods in Financial Engineering*. Applications of Mathematics. Springer, New York, NY, 2004.
- [24] Rémi Munos. Error bounds for approximate value iteration. In *Proceedings of the 20th National Conference on Artificial Intelligence (AAAI-05)*, volume 2, pages 1006–1011. AAAI Press, 2005.
- [25] Gabriel Peyré and Marco Cuturi. Computational optimal transport. *Foundations and Trends® in Machine Learning*, 11(5–6):355–607, 2019. doi: 10.1561/22000000073.
- [26] Open-Finance-Lab. Task 1: Finrl-deepseek for stock trading (finrl contest 2025 documentation). <https://huggingface.co/datasets/Zihan1004/FNSPID>, 2025. Retrieved July 12, 2025.

- [27] Andrew Ang, Robert J. Hodrick, Yuhang Xing, and Xiaoyan Zhang. The cross-section of volatility and expected returns. *The Journal of Finance*, 61(1):259–299, 2006. doi: 10.1111/j.1540-6261.2006.00836.x.
- [28] Zhaobo Zhu, Wenjie Ding, Yi Jin, and Dehua Shen. Dissecting the idiosyncratic volatility puzzle: A fundamental analysis approach. *Research in International Business and Finance*, 66:102085, 2023. doi: 10.1016/j.ribaf.2023.102085. URL <https://doi.org/10.1016/j.ribaf.2023.102085>.
- [29] Jiaxu Wang, Mo Hai, and Haifeng Li. A deep reinforcement learning model for portfolio management based on weight adjustment. *Procedia Computer Science*, 242:356–363, 2024. doi: 10.1016/j.procs.2024.08.174.
- [30] Xinyao Wang and Lili Liu. Risk-sensitive deep reinforcement learning for portfolio optimization. *Journal of Risk and Financial Management*, 18(7):347, 2025. doi: 10.3390/jrfm18070347.
- [31] Himanshu Choudhary, Arishi Orra, and Manoj Thakur. Finxplorer: An adaptive deep reinforcement learning framework for balancing and discovering investment opportunities, 2025. arXiv:2509.10531.
- [32] Victor DeMiguel, Lorenzo Garlappi, and Raman Uppal. Optimal versus naive diversification: How inefficient is the 1/n portfolio strategy? *The Review of Financial Studies*, 22(5):1915–1953, 2009. doi: 10.1093/rfs/hhm075.
- [33] Matteo Gelmini and Pierpaolo Uberti. The equally weighted portfolio still remains a challenging benchmark. *International Economics*, 179:100525, 2024. doi: 10.1016/j.inteco.2024.100525.
- [34] Harry Markowitz. Portfolio selection. *The Journal of Finance*, 7(1):77–91, 1952. doi: 10.1111/j.1540-6261.1952.tb01525.x.
- [35] Zhao-Rong Lai and Haisheng Yang. A survey on gaps between mean-variance approach and exponential growth rate approach for portfolio optimization. *ACM Computing Surveys*, 55(2):25:1–25:36, 2023. doi: 10.1145/3485274.
- [36] Denis B. Chaves, Jason Hsu, Feifei Li, and Omid Shakernia. Risk parity portfolio vs. other asset allocation heuristic portfolios. *The Journal of Investing*, 20(1):108–118, 2011. doi: 10.3905/joi.2011.20.1.108.
- [37] Hidehiko Shimizu and Takayuki Shiohama. Constructing inverse factor volatility portfolios: A risk-based asset allocation for factor investing. *International Review of Financial Analysis*, 68:101438, 2020. doi: 10.1016/j.irfa.2019.101438.
- [38] Olivier Ledoit and Michael Wolf. Honey, i shrunk the sample covariance matrix. *The Journal of Portfolio Management*, 30(4):110–119, 2004. doi: 10.3905/jpm.2004.110.
- [39] Olivier Ledoit and Michael Wolf. Analytical non-linear shrinkage of large-dimensional covariance matrices. *The Annals of Statistics*, 48(5):3043–3065, 2020. doi: 10.1214/19-AOS1921.
- [40] John Schulman, Philipp Moritz, Sergey Levine, Michael I. Jordan, and Pieter Abbeel. High-dimensional continuous control using generalized advantage estimation, 2015.
- [41] Christian Francq and Jean-Michel Zakoïan. Virtual historical simulation for estimating the conditional var of large portfolios. *Journal of Econometrics*, 217(2):356–380, 2020. doi: 10.1016/j.jeconom.2019.12.008.
- [42] Yingjie Fei, Zhuoran Yang, Yudong Chen, and Zhaoran Wang. Exponential bellman equation and improved regret bounds for risk-sensitive reinforcement learning. In *Advances in Neural Information Processing Systems (NeurIPS)*, 2021. URL <https://openreview.net/forum?id=IUqgofswxo>.
- [43] Leonid V Kantorovich and Gennady S Rubinstein. On a space of completely additive functions. *Vestnik Leningradskogo Universiteta*, 13(7):52–59, 1958.

A Additional Proofs

Definition A.1 (Induced continuation distributions). Fix a decision-time state ϕ and action a with executed control $\mathbf{w} = \Pi(a)$. Define the realized continuation distribution as

$$\begin{aligned}
 K_{\text{real}}(B \mid \phi, a) &:= \int \mathbf{1}\{E_B(\phi, \mathbf{w}, \mathbf{r})\} P_{\text{real}}(d\mathbf{r} \mid \phi), \\
 E_B(\phi, \mathbf{w}, \mathbf{r}) &:= (\text{Upd}(\phi, \mathbf{w}, \mathbf{r}) \in B).
 \end{aligned} \tag{23}$$

and the scenario-consistent continuation distribution by

$$\begin{aligned} K_{\text{scen}}(B \mid \phi, \psi, a) &:= \int \mathbf{1}\{E_B(\phi, \mathbf{w}, \mathbf{R})\} P_{\text{scen}}(d\mathbf{R} \mid \psi), \\ E_B(\phi, \mathbf{w}, \mathbf{R}) &:= (\text{Upd}(\phi, \mathbf{w}, \mathbf{R}) \in B). \end{aligned} \quad (24)$$

for any measurable set B in the state space.

A.1 Proof of Lemma 3.1

Proof. Fix ϕ and a policy π . By definition,

$$(T_{\text{hyb}}^\pi V)(\phi) = \mathbb{E}[r(\phi, \mathbf{w}; \mathbf{R}) + \delta V(\text{Upd}(\phi, \mathbf{w}, \mathbf{r})) \mid \phi],$$

where $a \sim \pi(\cdot \mid \phi)$, $\mathbf{w} = \Pi(a)$, $\mathbf{R} \sim P_{\text{scen}}(\cdot \mid \psi)$ and $\mathbf{r} \sim P_{\text{real}}(\cdot \mid \phi)$. Similarly,

$$(T_{\text{scen}}^\pi V)(\phi) = \mathbb{E}[r(\phi, \mathbf{w}; \mathbf{R}) + \delta V(\text{Upd}(\phi, \mathbf{w}, \mathbf{R})) \mid \phi].$$

Subtracting, the reward terms cancel since both operators evaluate $r(\phi, \mathbf{w}; \cdot)$ on the same scenario draw \mathbf{R} :

$$\begin{aligned} \Delta^\pi V(\phi) &:= (T_{\text{hyb}}^\pi V - T_{\text{scen}}^\pi V)(\phi), \\ \phi^+(\phi, a, x) &:= \text{Upd}(\phi, \Pi(a), x). \end{aligned}$$

$$\begin{aligned} \Delta^\pi V(\phi) &= \delta \mathbb{E}_{a \sim \pi(\cdot \mid \phi)} [\Delta_V(\phi, \psi, a)], \\ \Delta_V(\phi, \psi, a) &:= \mathbb{E}_{\mathbf{r}} V(\phi^+(\phi, a, \mathbf{r})) - \mathbb{E}_{\mathbf{R}} V(\phi^+(\phi, a, \mathbf{R})). \end{aligned} \quad (25)$$

Using the induced continuation distributions $K_{\text{real}}(\cdot \mid \phi, a)$ and $K_{\text{scen}}(\cdot \mid \phi, \psi, a)$ from Definition A.1, rewrite

$$\mathbb{E}_{\mathbf{r}} V(\text{Upd}(\phi, \Pi(a), \mathbf{r})) = \int V(\phi') K_{\text{real}}(d\phi' \mid \phi, a). \quad (26)$$

$$\mathbb{E}_{\mathbf{R}} V(\text{Upd}(\phi, \Pi(a), \mathbf{R})) \quad (27)$$

$$= \int V(\phi') K_{\text{scen}}(d\phi' \mid \phi, \psi, a). \quad (28)$$

Therefore

$$\begin{aligned} \pi_\phi &:= \pi(\cdot \mid \phi), \\ \Delta K_{\phi, \psi, a}(d\phi') &:= K_{\text{real}}(d\phi' \mid \phi, a) - K_{\text{scen}}(d\phi' \mid \phi, \psi, a), \\ \langle V, \Delta K_{\phi, \psi, a} \rangle &:= \int V(\phi') \Delta K_{\phi, \psi, a}(d\phi'). \end{aligned}$$

where $\Delta K := K_{\text{real}} - K_{\text{scen}}$. If $P_{\text{real}}(\cdot \mid \phi) = P_{\text{scen}}(\cdot \mid \psi)$, then $K_{\text{real}} = K_{\text{scen}}$ and the difference is zero. If $\text{Upd}(\phi, \mathbf{w}, \cdot)$ is outcome-independent, then both induced kernels coincide as well. \square

A.2 Proof of Proposition 3.2

Proof. Fix ϕ . Fix an o such that $\Phi(o) = \phi$, and set $\psi := \Psi(o)$. By Lemma 3.1,

$$\begin{aligned} m_{\text{real}}(\phi, a) &:= \mathbb{E}_{\mathbf{r} \sim P_{\text{real}}(\cdot \mid \phi)} f_{\phi, a}(\mathbf{r}), \\ m_{\text{scen}}(\phi, \psi, a) &:= \mathbb{E}_{\mathbf{R} \sim P_{\text{scen}}(\cdot \mid \psi)} f_{\phi, a}(\mathbf{R}). \end{aligned}$$

Let

$$\Delta^\pi V(\phi) := (T_{\text{hyb}}^\pi V - T_{\text{scen}}^\pi V)(\phi).$$

Then

$$\Delta^\pi V(\phi) = \delta \mathbb{E}_{a \sim \pi(\cdot \mid \phi)} [m_{\text{real}}(\phi, a) - m_{\text{scen}}(\phi, \psi, a)]$$

where $f_{\phi, a}(\mathbf{x}) := V(\text{Upd}(\phi, \Pi(a), \mathbf{x}))$.

By assumption, $\mathbf{x} \mapsto \text{Upd}(\phi, \Pi(a), \mathbf{x})$ is L_h -Lipschitz through the outcome-updated memory component and V is L_V -Lipschitz in that component, hence $f_{\phi, a}$ is $(L_V L_h)$ -Lipschitz under $\|\cdot\|_2$. By Kantorovich–Rubinstein duality for W_1 (with cost $d(\mathbf{x}, \mathbf{y}) = \|\mathbf{x} - \mathbf{y}\|_2$) [43],

$$P_{\text{real}}^\phi := P_{\text{real}}(\cdot \mid \phi), \quad P_{\text{scen}}^\psi := P_{\text{scen}}(\cdot \mid \psi).$$

$$\left| \mathbb{E}_{\mathbf{r}} f_{\phi, a}(\mathbf{r}) - \mathbb{E}_{\mathbf{R}} f_{\phi, a}(\mathbf{R}) \right| \leq (L_V L_h) W_1(P_{\text{real}}^\phi, P_{\text{scen}}^\psi).$$

Taking expectation over $a \sim \pi(\cdot \mid \phi)$, multiplying by δ , and then taking the supremum over o yields

$$\Delta_W := \sup_o W_1(P_{\text{real}}(\cdot \mid \Phi(o)), P_{\text{scen}}(\cdot \mid \Psi(o))).$$

$$\|T_{\text{hyb}}^\pi V - T_{\text{scen}}^\pi V\|_\infty \leq \delta L_V L_h \Delta_W. \quad \square$$

A.3 Proof of Corollary 3.3

Proof. Let V_{hyb}^π and V_{scen}^π be the fixed points of T_{hyb}^π and T_{scen}^π . Since both operators are δ -contractions in $\|\cdot\|_\infty$,

$$\begin{aligned} \|V_{\text{hyb}}^\pi - V_{\text{scen}}^\pi\|_\infty &= \|T_{\text{hyb}}^\pi V_{\text{hyb}}^\pi - T_{\text{scen}}^\pi V_{\text{scen}}^\pi\|_\infty \\ &\leq \|T_{\text{hyb}}^\pi V_{\text{hyb}}^\pi - T_{\text{hyb}}^\pi V_{\text{scen}}^\pi\|_\infty \\ &\quad + \|(T_{\text{hyb}}^\pi - T_{\text{scen}}^\pi) V_{\text{scen}}^\pi\|_\infty. \end{aligned}$$

The first term is at most $\delta \|V_{\text{hyb}}^\pi - V_{\text{scen}}^\pi\|_\infty$ by contraction. Rearranging gives

$$\|V_{\text{hyb}}^\pi - V_{\text{scen}}^\pi\|_\infty \leq \frac{1}{1 - \delta} \|(T_{\text{hyb}}^\pi - T_{\text{scen}}^\pi) V_{\text{scen}}^\pi\|_\infty.$$

Apply Proposition 3.2 with $V = V_{\text{scen}}^\pi$ to obtain (20). \square

A.4 Proof of Theorem 3.5

Proof. Fix (ϕ, ψ, a) and write $\mathbf{w} = \Pi(a)$. Define

$$f(\mathbf{x}) := V_{\text{scen}}^\pi(\text{Upd}(\phi, \mathbf{w}, \mathbf{x})).$$

By Assumption 3.4, $\mathbf{x} \mapsto \text{Upd}(\phi, \mathbf{w}, \mathbf{x})$ is L_h -Lipschitz through the outcome-updated memory component and V_{scen}^π is L_V -Lipschitz in that component, hence f is $(L_V L_h)$ -Lipschitz under $\|\cdot\|_2$.

Let $\mathbf{R} \sim P_{\text{scen}}(\cdot | \psi)$, $\mathbf{r} \sim P_{\text{real}}(\cdot | \phi)$, and $\mu_\psi = \mathbb{E}[\mathbf{R} | \psi]$. Since both Y^* and $Y_{\beta_{\text{cf}}}$ use the same reward term $r(\phi, \mathbf{w}; \mathbf{R})$, the deviation enters only via continuation:

$$\begin{aligned} Y_r - Y^* &= \delta(f(\mathbf{r}) - f(\mathbf{R})), \\ Y_c - Y^* &= \delta(f(\mu_\psi) - f(\mathbf{R})). \end{aligned}$$

Let $\beta = \beta_{\text{cf}}$ and $\alpha = 1 - \beta$. Then

$$Y_\beta - Y^* = \alpha(Y_r - Y^*) + \beta(Y_c - Y^*).$$

Using $(u + v)^2 \leq 2u^2 + 2v^2$ yields

$$(Y_\beta - Y^*)^2 \leq 2\alpha^2(Y_r - Y^*)^2 + 2\beta^2(Y_c - Y^*)^2.$$

Taking conditional expectations,

$$\begin{aligned} \mathbb{E}[(Y_\beta - Y^*)^2 | \phi, \psi, a] &\leq 2\alpha^2 \mathbb{E}[(Y_r - Y^*)^2 | \phi, \psi, a] \\ &\quad + 2\beta^2 \mathbb{E}[(Y_c - Y^*)^2 | \phi, \psi, a]. \end{aligned} \tag{29}$$

For the realized-continuation term, let γ^* be an optimal coupling of $P_{\text{real}}(\cdot | \phi)$ and $P_{\text{scen}}(\cdot | \psi)$, so that

$$\Delta_2(\phi, \psi) = W_2^2(P_{\text{real}}(\cdot | \phi), P_{\text{scen}}(\cdot | \psi)) = \mathbb{E}_{\gamma^*}[\|\mathbf{r} - \mathbf{R}\|_2^2].$$

By Lipschitzness of f ,

$$|f(\mathbf{r}) - f(\mathbf{R})| \leq (L_V L_h) \|\mathbf{r} - \mathbf{R}\|_2,$$

hence

$$\begin{aligned} \mathbb{E}[(Y_r - Y^*)^2 | \phi, \psi, a] &= \delta^2 \mathbb{E}[(f(\mathbf{r}) - f(\mathbf{R}))^2 | \phi, \psi, a] \\ &\leq \delta^2 (L_V L_h)^2 \Delta_2(\phi, \psi). \end{aligned}$$

For the proxy-continuation term, by Lipschitzness,

$$|f(\mu_\psi) - f(\mathbf{R})| \leq (L_V L_h) \|\mu_\psi - \mathbf{R}\|_2,$$

so

$$\begin{aligned} \mathbb{E}[(Y_c - Y^*)^2 | \phi, \psi, a] &= \delta^2 \mathbb{E}[(f(\mu_\psi) - f(\mathbf{R}))^2 | \phi, \psi, a] \\ &\leq \delta^2 (L_V L_h)^2 \mathbb{E}[\|\mathbf{R} - \mu_\psi\|_2^2 | \psi] \\ &= \delta^2 (L_V L_h)^2 \sigma_{\text{scen}}^2(\psi). \end{aligned}$$

Substitute into (29) to obtain (21). \square

A.5 Proof of Corollary 3.6

Proof. We derive the optimal mixing weight by minimizing

$$g(\beta) := (1 - \beta)^2 A(\phi, \psi) + \beta^2 B(\psi), \quad \beta \in [0, 1].$$

Upon expansion, we obtain $g(\beta) = A(\phi, \psi) - 2A(\phi, \psi)\beta + (A(\phi, \psi) + B(\psi))\beta^2$. Next, we differentiate this expression and set the derivative equal to zero:

$$\begin{aligned} g'(\beta) &= -2A(\phi, \psi) + 2(A(\phi, \psi) + B(\psi))\beta = 0, \\ \Rightarrow \beta^* &= \frac{A(\phi, \psi)}{A(\phi, \psi) + B(\psi)}. \end{aligned}$$

Given that both $A(\phi, \psi)$ and $B(\psi)$ are non-negative, it follows that $\beta^* \in [0, 1]$. \square